

MODELING OF A NON-STATIONARY PROCESS OF GAS OUTFLOW
INTO A OPENED AREA FILLED WITH LIQUID
WITH A TUBE ARRAY

Alekseev M.V. ¹, Lezhnin S.I. 

Abstract In a two-dimensional formulation, a numerical simulation of the process of the outflow of an air stream into a liquid-filled area in which a staggered tube array was located was carried out. In this case, liquids with significantly different densities (water, heavy liquid metal) were considered. It is shown that the process of displacement of liquid by a gas cavity in such an area for liquid metal and water occurs in a similar way.

The main difference between the outflow of gas into liquid metal and water is associated with the expansion rate of the gas cavity. The rate of cavity expansion in liquid metal is less than in water.

It is shown that during the outflow process, gas-dynamic structures of velocity jumps are formed inside the gas cavity between the nozzle and the first row of the tube array. When flowing into liquid metal, a similar gas-dynamic structure is less pronounced. The emergence of vortex structures behind the upper row of the tube array when liquid flows into the upper free volume has been revealed.

Key words: OpenFOAM, VOF, tube array, gas outflow in liquid.

AMS Mathematics Subject Classification: 76B10.

DOI: 10.32523/2306-6172-2025-13-1-17-25

1 Introduction

A detailed study of the behavior of gas jets during critical flow into a liquid began actively in the 70s of the last century [1]. The results of the latest experimental and computational studies are presented in [2, 3, 4]. The formation of complex flow structures and gas jets when flowing into a liquid is determined by the inertia of the external environment, the density of which (for water) is 800 times higher than the density of air. A gas cavity appears near the nozzle, inside which a gas-dynamic structure of shock waves is established. Instabilities of the Kelvin–Helmholtz and Rayleigh–Taylor types develop on the surface of the gas cavity. As a result, gas bubbles and water droplets are generated at the interface. Far from the nozzle, the gas cavity can break up into a bubble cluster when large bubbles fragment. This is an incomplete class of phenomena that occurs for gas jets at a critical outflow into a free volume.

The density of the liquid into which the gas escapes can be significantly higher than the density of water (for example, a heavy liquid metal). Because of this, the role of inertial and gravitational effects during the outflow of a gas jet significantly increases. The internal space filled with liquid in metallurgical, power engineering and hydrogen (see, for example [5]) production equipment can have complex geometry: channels, spacer grids, nozzles, tube

¹Corresponding Author.

sheets, etc. Therefore, the role of wall effects on the solid wall increases (friction, wettability, stagnant zones, pressure surges due to flow deceleration), which fundamentally distinguishes the process under study from the outflow of a gas jet into a free volume filled with liquid.

In earlier works, the authors numerically studied the processes of gas outflow into an open pipe region filled with liquid (water, liquid metal) at high pressure drops ($\Delta P = 1.6$ MPa). Calculations were carried out both in the axisymmetric two-dimensional formulation [6] and in the three-dimensional one [7]. It was shown that when flowing into water, a jet gas cavity was formed inside which a gas-dynamic structure of shock waves was established. Unlike water, in liquid metal the air cavity increases in size, both in height and width due to large inertial and gravitational forces in the liquid metal. A comparison of two-dimensional calculation and three-dimensional one showed that the two-dimensional calculation allows, to a first approximation, a good description of the pressure dynamics and hydrodynamic characteristics.

In subsequent works, the authors carried out modeling of gas outflow in a two-dimensional formulation: a) when there were obstacles in the liquid volume in the form of ring channels [8]; b) when the obstacle in the form of a disk was at different distances from the nozzle [9]. It was shown that for the annular assembly [8] the gas flows out in the form of annular gas cavities. The presence of a disk barrier [9] inside the volume in the liquid lead to the formation of a gas cavity between the disk and the nozzle. At the same time, the cavity began to fragment behind the barrier.

The presence of tube sheets inside the area filled with a liquid makes the calculation problem closer to the real behavior of a two-phase mixture in various technical devices. Tube sheets can significantly change the flow of gas into liquids of different densities. It is also important to calculate the force impact on the elements of the tube sheet.

The purpose of this work is a detailed study of the unsteady process of gas (air) injection into an open pipe region partially filled with liquid (water or liquid metal) in the presence of a “chessboard” tube array inside.

2 Methods

In this work, a two-dimensional, flat problem of air flow into a region filled with liquid (liquid metal, water) was solved in the presence of a “chessboard” array of tubes inside (Fig. 1). The width of working volume 1 was $D = 0.2$ m and height $H = 0.5$ m. The liquid level was set at a height of $h = 0.4$ m. The upper part of the volume was filled with air. The initial pressure in the working area was $P = 2$ MPa. The gas exited into the working volume through pipe 2 at the bottom of the working area. Branch pipe 2 was connected to receiver volume 3. The width of the pipe was $d_1 = 0.02$ m and length $L = 0.1$ m. Receiver volume 3 was width $d = 0.1$ m and length $L = 0.1$ m. Initial air pressure in the pipe and in the receiver the volume was $P = 18$ MPa.

On the upper face of volume 1 (*outlet*), a boundary condition was set for free inflow and outflow at constant pressure. For velocity U , this boundary condition was specified as $\partial U / \partial n = 0$ for outflow, and for inflow it was set relative to the boundary $U = U_n$ (calculated from the speed in the border cell). The pressure was considered constant $P = 2$ MPa. The boundary condition for the volumetric fluid content is $\partial \alpha / \partial n = 0$, and for temperature $-\partial T / \partial n = 0$.

At the lower boundary (*inlet*) of receiver volume 3, the condition of free inflow-outflow at constant pressure was also set. The speed U is set to $\partial U / \partial n = 0$ for outflow, for inflow $U = U_n$ (calculated from the speed in the border cell). The pressure was considered constant $P = 18$ MPa. The boundary condition for the volumetric liquid content is $\alpha = 0$ (gas flow),

Table 1: Thermophysical properties of phases.

	Water ($T = 585.55$ K)	Air ($T = 650$ K)	Liquid metal ($T = 650$ K)
ρ , kg/m ³	849.79	1.206	11341
μ , Pa · c	$0.1261 \cdot 10^{-3}$	$1.84 \cdot 10^{-5}$	$2.53 \cdot 10^{-3}$
C_p , J/kg	4565	1050	151
σ , N/m	0.07274	< - - >	0.44815

the range (0, 1) at the gas/liquid interface. The work solved two problems: air injection into water and air injection into liquid metal. The properties of the phases are indicated in the Tab. 1.

The dynamics and heat transfer of a two-phase medium were determined by the equations of continuity (1), momentum (2) and energy (3):

$$\frac{\partial \rho}{\partial t} + \nabla \cdot (\rho \vec{U}) = 0, \quad (1)$$

$$\frac{\partial \rho \vec{U}}{\partial t} + \nabla \cdot (\vec{U} \rho \vec{U}) = -\nabla \left(p + \frac{2}{3} \mu_{eff} \nabla \vec{U} \right) + \left[\nabla (\mu_{eff} \nabla \vec{U}) + (\nabla \vec{U} \cdot \nabla \mu_{eff}) \right] + \rho \vec{g} + \vec{f}_s, \quad (2)$$

$$\frac{\partial \rho T}{\partial t} + \nabla \cdot (\rho \vec{U} T) + \left(\frac{\alpha}{C_{V,l}} + \frac{1-\alpha}{C_{V,g}} \right) \left(\frac{\partial \rho K}{\partial t} + \nabla (\rho \vec{U} K) + \nabla (\vec{U} p) \right) = \nabla \alpha_{eff} \nabla T. \quad (3)$$

Here \vec{U} is the local velocity vector, t is time, ρ is density, p is pressure, $C_{V,g}$ and $C_{V,l}$ are isochoric heat capacity gas and liquid, respectively, T – temperature, $\alpha_{eff} = (\lambda_l + \lambda_{turb,l})\alpha_l / C_{p,l} + (\lambda_g + \lambda_{turb,g})\alpha_g / C_{p,g}$ – coefficient of effective turbulent diffusion of the mixture, $\lambda_{l,g}$ – thermal conductivity coefficients of each phase, $C_{p,g}$ and $C_{v,l}$ are isobaric heat capacity of gas and liquid respectively, $g = 9.81$ m/s² – acceleration of free fall, $K = |\vec{U}|^2/2$ – specific kinetic energy. The effective dynamic viscosity $\mu_{eff} = \mu + \nu_t \rho$ was determined in terms of viscosity and turbulent viscosity. The surface tension force in the equation (2) at the liquid–gas interface was determined using the continuous surface force (CSF) model [12]: $f_s = \sigma k_s n$, where σ is the surface tension coefficient tension, k_s is the curvature of the free surface, which is defined as the divergence of the normal vector: $k_s = \nabla (\nabla \alpha / |\nabla \alpha|)$. The normal to the free surface was calculated as the gradient of the volume fraction of the liquid phase in the cell: $n = \nabla \alpha$. The transport equation for the volume fraction of liquid, a two-phase compressible flow, is written in the following form:

$$\frac{\partial \alpha}{\partial t} + \nabla (\alpha \vec{U}_l) + \nabla \left(\alpha (1 - \alpha) \vec{U}_r \right) = \alpha (1 - \alpha) \left(\frac{\psi_g}{\rho_g} - \frac{\psi_l}{\rho_l} \right) \frac{Dp}{Dt} + \alpha \nabla \vec{U}, \quad (4)$$

where $\vec{U}_r = \vec{U}_l - \vec{U}_g$ is the phase slip speed, $\vec{U} = \alpha \vec{U}_l + (1 - \alpha) \vec{U}_g$ – velocity vector expressed in terms of phase velocities, Ψ_g, Ψ_l – compressibility, respectively for gas and liquid.

The closure of the equations was carried out using the equations of state for each of the phases $\rho_{l,g}(p, T) = \rho_{0,l,g} + \Psi_{l,g}(T) \cdot p$, where $\Psi_{l,g}(T)$ is the compressibility of each phase, $\rho_{0,l,g}$ is the nominal density. For the compressible phase (i.e. gas), the nominal density is $\rho_{0,g} = 0$ and $\Psi_g(T) = 1/R_\mu T$, which leads to the ideal equation of state gas $\rho_g(p, T) = \Psi_{l,g}(T) \cdot p = p/R_\mu T = p\mu/RT$, where R is the gas constant, μ – molar mass. For a phase with low compressibility (i.e. liquid), the nominal density of the liquid under normal conditions is set to $\rho_{0,l} = const$, the compressibility is determined by $\Psi_g = 1/c^2$, where c – speed of sound.

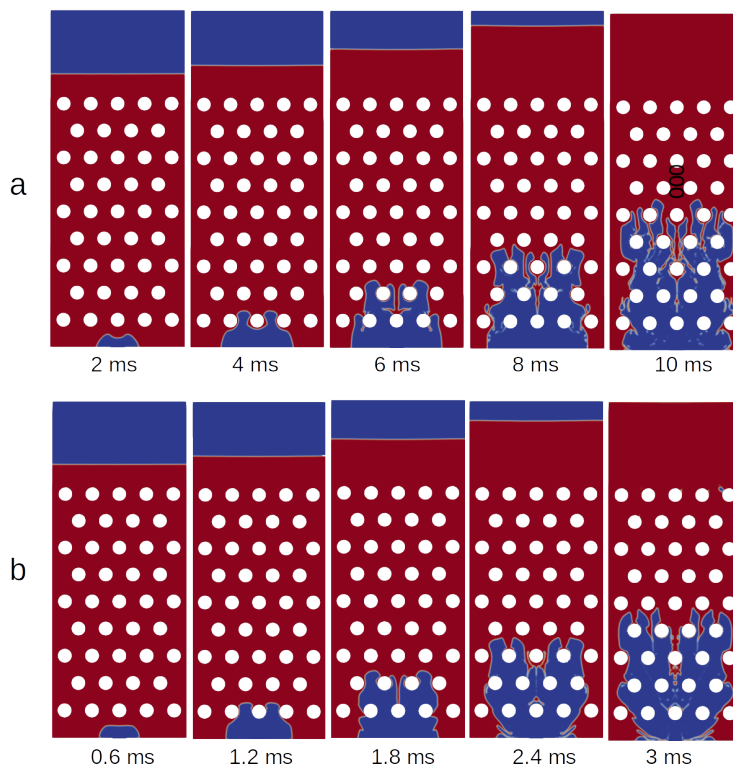


Figure 2: Distribution of volumetric content for liquid metal (a) and water (b) at different times, red color is liquid, blue color is air.

The two-phase flow model was complemented by the URANS (Unsteady Reynolds-averaged Navier–Stokes equations) turbulence model k – ω SST (shear-stressed transport), which is a combination of k – ϵ and k – ω turbulence models. The F_1 mixing function activates the k – ω model, which is well suited for simulating flow in a viscous sublayer, and the k – ϵ model, which is ideal for simulating flow in regions remote from the wall. This ensures that the appropriate model is used throughout the entire [10] flow field.

Boundary conditions at the inlet and outlet boundaries for the turbulent kinetic energy k were set as $\partial k / \partial n = 0$. On the same faces, the condition for the specific dissipation rate ω was set as $\partial \omega / \partial n = 0$. On the walls (faces *wall*), standard wall functions were specified on k and ω .

The physical and mathematical model of the compressibleInterFoam solver of the OpenFOAM code was tested by the authors on a variety of problems related to the flow of two-phase flows [15, 16, 17, 18]. Fig. 1 shows the geometry of the computational grid. The mesh was uniform with a cell width of 1 mm. There was double thinning near the walls; the width of the minimum cell was 0.016 mm. The total number of cells was $340 \cdot 10^3$. In previous works [19, 20], calculations with similar two-dimensional geometry and mesh (number of cells $50 \cdot 10^3$) cross-verification was carried out with calculations on a one-dimensional process model and three-dimensional ones on grids there are more than $1.3 \cdot 10^6$ cells. It was shown that two-dimensional calculations provide a good approximation from one-dimensional to three-dimensional detail of the process of gas outflow in liquids with different densities. Two-dimensional calculation allows us to determine the evolution of pressure and the rate of change in the volume of a gas cavity in a liquid with minimal methodological error and low computational costs.

3 Results

Fig. 2 (a) and 2 (b) show the distribution of the volumetric content of liquid metal and water at different times, respectively. It can be noted that when gas flows into liquid metal (Fig. 2 (a)) within a time of 3 ms, a gas cavity forms in the lower part of the volume. By the time of 4 ms, the cavity boundary reaches the first row of the tube sheet and then goes around the three pipes of the first row. At 6 ms, the cavity boundary reaches the second row, at 8 ms the third, and at 10 ms the fourth and fifth rows. With each subsequent passage of the cavity boundary through a row of tube sheet, the boundary is fragmented into jets. By the time of 10 ms, the upper gas volume is completely displaced by liquid metal. When gas flows into water (Fig. 2 (b)), the process of displacement of the upper gas volume occurs in 3 ms. The formation of a gas cavern in the lower part of the volume occurs in 0.8–1.0 ms, the cavity boundary reaches the first row at 1.2 ms, the second row at 1.8 ms, the third at 2.4 ms, and the fourth at 3 ms. It can be noted that, despite the significant difference in the density of liquid metal and water, the geometry of the gas cavity growth process in a staggered tube sheet is similar, which was not observed for an open tube geometry without a tube sheet [6, 7]. In the absence of a tube sheet, the outflow of gas into water occurred in the form of a jet, and the outflow of gas into liquid metal in the form of a “slug” gas cavity.

Fig. 3 shows the distribution of the velocity modulus at different times during the flow of gas into metal (a) and into water (b). It can be noted that when a gas cavity is formed between the nozzle and the first row of the tube sheet, a gas–dynamic structure of velocity jumps appears. For gas flowing into liquid metal, the maximum speed was 400 m/s; for gas flowing into water, it was 730 m/s. In the upper, last row of the tube sheet, a stagnation zone is formed behind each pipe; the liquid exits into the upper free space in the form of jets between the pipes. This condition leads to the formation of vortex structures behind the last upper row of pipes. Fig. 4 shows streamlines at different times during the flow of gas into liquid metal (a) and the flow of gas into water (b). At the initial moments of time, during the formation of a gas cavity, a symmetrical vortex structure is formed inside it, near the nozzle (Fig. 4 (a) time point 6 ms, Fig. 4 (b) time point 1.8 ms). Next, this vortex structure inside the gas cavity disintegrates into many unstable vortex structures. When a liquid is displaced inside a staggered tube grid, the movement of the liquid is irrotational – the flow lines go around the tubes of the staggered grid. By the time of 8 ms, when gas flows into liquid metal, vortex structures form behind the last, upper row of the tube sheet when liquid flows into the upper free volume. For water, by the time of 2.4 ms, the formation of vortex structures behind the last row of tube sheets also occurs.

4 Conclusion

In a two–dimensional formulation, a numerical simulation of the process of the outflow of a stream of air into a liquid–filled area in which a staggered tube array was located was carried out. In this case, liquids with significantly different densities (water, metal) were considered. It is shown that the process of displacement of liquid by a gas carpet in such an area for liquid metal and water occurs in a similar way. The main difference between the outflow of gas into liquid metal and water is associated with the expansion rate of the gas cavity. The rate of cavity expansion in liquid metal is approximately 3.3 times less than in water.

The formation of gas–dynamic structures of velocity jumps inside the gas cavity between the nozzle and the first row of the tube sheet is shown. When flowing into liquid metal, the gas–dynamic structure is less pronounced. The emergence of vortex structures behind the

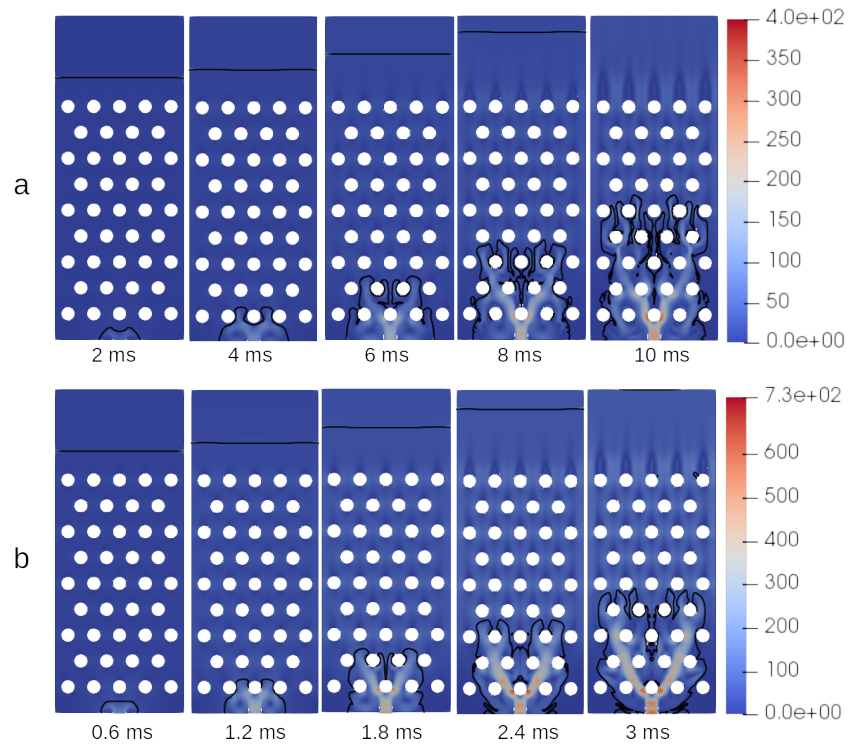


Figure 3: Distribution of the velocity modulus for liquid metal (a) and water (b) at different times, black contour is the location of the interphase boundary.

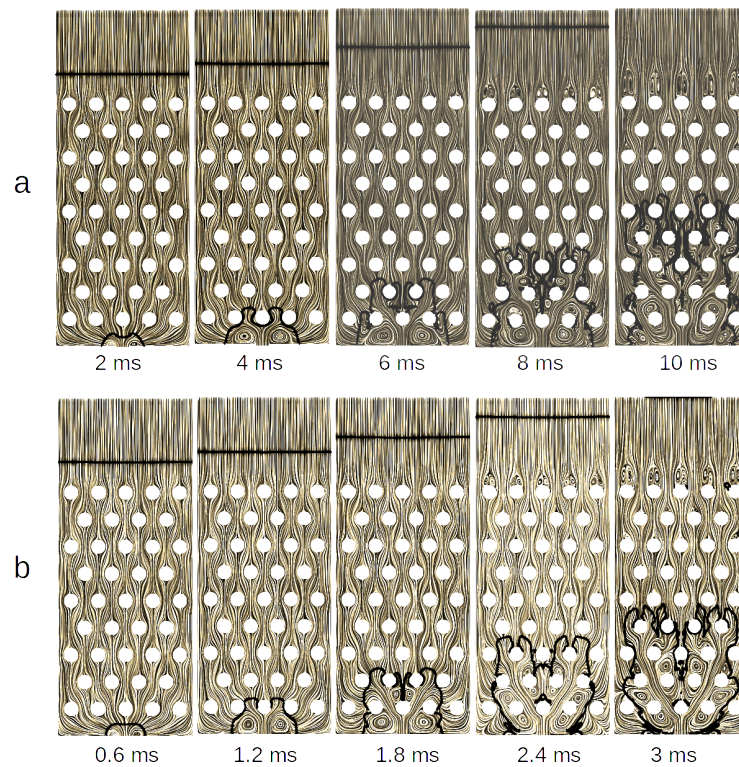


Figure 4: Streamlines for liquid metal (a) and water (b) at different times, black contour – location of the interface.

upper row of the tube sheet when liquid flows into the upper free volume has been revealed.

Acknowledgement

The work was supported by a state contract of the Russian Federation with the Institute of Thermophysics SB RAS (121032200034–4)

References

- [1] Chawla T.C., *Droplet size resulting from breakup of liquid at gas–liquid interfaces of liquid–submerged subsonic and sonic gas jets*, Int. J. Multiph. Flow, 2 (1975), 471–475.
- [2] Zhang X., Li Sh., Yang B. and Wang N., *Flow structures of over–expanded supersonic gaseous jets for deep-water propulsion*, Ocean Engineering, 213. (2020), 107611.
- [3] Zhang X., Li Sh., Yu D., Yang B. and Wang N., *The Evolution of Interfaces for Underwater Supersonic Gas Jets*, Water, 12. 2 (2020), 488.
- [4] Leon M.G., Valencia A.M., *Analysis of submerged single and twin gas jet injection using URANS–CFD simulations*, Eur. J. Mech. B/Fluids., 90. (2021), 114–127.
- [5] Geibler T., Stoppel L., Wetzl Th. et al., *Experimental investigation and thermo–chemical modeling of methane pyrolysis in a liquid metal bubble column reactor with a packed bed*, Int. J. Hydrogen Energy, 40. 41 (2015), 14134–14146.
- [6] Lezhnin S. I., Alekshev M. V. and Vozhakov I. S., *Modeling the dynamics of gas (steam) outflow into a high–density liquid taking into account interfacial heat exchange*, J. Phys. Conf. Ser., 1128. (2018), 012037.
- [7] Alekshev M. V., Vozhakov I.S., Lezhnin S. I. and Pribaturin N. A., *Three–dimensional simulation of gas injection into an open fluid–filled pipe region*, J. Phys. Conf. Ser., 1382. (2019), 012071.
- [8] Alekshev M.V., Lezhnin S.I., *Simulation of an unstationary process of gas outflow into an open pipe area with a ring assembly filled with a liquid*, J. Phys. Conf. Ser., 2057. 1 (2021), 012038.
- [9] Vozhakov I.S., Lezhnin S.I., *Numerical simulation of the process of gas outflow into an open pipe with an obstacle filled with a liquid (water, lead)*, J. Phys. Conf. Ser., 2057. 1 (2021), 012073.
- [10] Menter F.R., Kuntz M. and Langtry R., *Ten years of industrial experience with the SST turbulence model*, Turbulence, heat and mass transfer, 4. 1 (2003), 625–632.
- [11] The OpenFOAM Foundation, *Open source computational fluid dynamics (cfd) toolbox*, URL:openfoam.org, 2020.
- [12] Brackbill J.U., Kothe D.B. and Zemach C., *A continuum method for modeling surface tension*, J. Comput. Phys., 100. 2 (1992), 335–354.
- [13] Savchenko I.V., Lezhnin S.I. and Mosunova N.A., *Recommendations on adopting the values and correlations for calculating the thermophysical and kinetic properties of liquid lead*, Thermal Engineering, 62. (2015), 434–437.
- [14] Karmokov A.M., Dyshekova A.H. and Molokanova O.O., *Measurements of the contact angle of lead for surfaces of the iron oxide and reactor steel EI–852*, Applied Physics, 3. (2017), 85–88. (russian)
- [15] Alekshev M.V., Vozhakov I.S., *3D numerical simulation of hydrodynamics and heat transfer in the Taylor flow*, J. Engng Ther.Phys., 31. 2 (2022), 299–308.
- [16] Alekshev M.V, Lukyanov A.A. and Vozhakov I.S., *Numerical simulation of a Taylor bubble in a heated tube*, Interfacial Phenomena and Heat Transfer, 11. 2 (2023), 65–79.
- [17] Alekshev M. V., Lukyanov An. A., *Numerical simulation of a stationary Taylor gas bubble*, Thermophysics and Aeromechanics, 30. 2 (2023), 279–292.
- [18] Kashinsky O.N., Alekshev M.V., Lukyanov An.A., Kurdyumov A.S. and Lobanov P.D., *Investigation of the hydrodynamic characteristics of a stationary Taylor bubble at different speeds of the liquid downflow*, Thermophysics and Aeromechanics, 31. 3 (2024), 569–585. (russian)

- [19] Alekseev M. V., Vozhakov I. S. and Lezhnin S. I., *Pressure pulsations during gas injection into a liquid-filled closed vessel with a high pressure drop*, Thermophysics and Aeromechanics. 26. 5 (2019), 781–784.
- [20] Alekseev M.V., Vozhakov I.S. and Lezhnin S.I., *Non-stationary process characteristics of the gas outflow into a liquid*, Multiphase Systems, 14. 2 (2019), 82–88. (russian)

Maksim V. Alekseev,
Kutateladze Institute of Thermophysics SB RAS,
Russia, 630090, Novosibirsk, Lavrentyev ave., 1
Email: almaxcom@mail.ru,

Sergey I. Lezhnin,
Kutateladze Institute of Thermophysics SB RAS,
Russia, 630090, Novosibirsk, Lavrentyev ave., 1
Email: lezhnin@itp.nsc.ru.

Received 08.08.2024 , Accepted 15.01.2025, Available online 31.03.2025.